Coexistence of superconductivity and ferromagnetism in polycrystalline UGe_2

2001 J. Phys.: Condens. Matter 13 L759

(http://iopscience.iop.org/0953-8984/13/33/102)

INSTITUTE OF PHYSICS PUBLISHING JOURNAL OF PHYSICS: CONDENSED MATTER

J. Phys.: Condens. Matter **13** (2001) L759–L770 PII: S0953-8984(01)22378-9

LETTER TO THE EDITOR

Coexistence of superconductivity and ferromagnetism in polycrystalline UGe_2

E D Bauer, R P Dickey, V S Zapf and M B Maple

Department of Physics and Institute For Pure and Applied Physical Sciences, University of California, San Diego, La Jolla, CA 92093, USA

Received 1 March 2001, in final form 29 May 2001
Published 2 August 2001
Online at stacks.iop.org/JPhysCM/13/L759

Abstract

Electrical resistivity measurements have been made under nearly hydrostatic pressure up to 18 kbar and at temperatures between 50 mK and room temperature on polycrystalline specimens of the ferromagnetic compound UGe_2. The Curie temperature decreases monotonically with pressure and can no longer be identified from the electrical resistivity measurements at a critical pressure $P_c \simeq 16$ kbar. Plots of $d\rho/dT$ versus T reveal a feature in the $\rho(T)$ curves at $T_0 \sim 0.6T_C$ at $P = 0$ kbar that decreases monotonically with pressure and appears to vanish near P_c. The onset of superconductivity is observed in the range 8 kbar $< P <$ 14 kbar with a maximum onset temperature of 1.2 K at $P \sim 13$ kbar. The polycrystalline specimens have a residual resistivity ρ_0 up to $\sim 3\ \mu\Omega$ cm corresponding to an electron mean free path smaller than or of the order of the superconducting coherence length. These results suggest that high-purity specimens with long mean free paths are not necessary, at least in the case of UGe_2, in order to observe superconductivity near the critical pressure where the magnetic ordering temperature vanishes.

1. Introduction

Within the past few years, superconductivity under pressure P has been observed in high-purity single-crystal specimens of three magnetically ordered f-electron compounds in the vicinity of the critical pressure P_c at which the magnetic order vanishes. Two of these are the antiferromagnetic Ce compounds, $CeIn_3$ and $CePd_2Si_2$ [1], each of which has a Néel temperature T_N of $\sim$10 K, and the ferromagnetic material, UGe_2, which has a Curie temperature T_C of 55 K. The $CeIn_3$ [2] and $CePd_2Si_2$ [3] compounds exhibit superconductivity over a range of pressure of $\sim$6 kbar centred about the pressure where the superconducting critical temperature T_{SC} attains maximum values of $\sim$0.4 K and $\sim$0.2 K, respectively, close to the values of pressure where T_N extrapolates to zero ($P_c \sim 26$ kbar and 28 kbar for $CeIn_3$ and $CePd_2Si_2$, respectively). The UGe_2 compound displays superconductivity over a pressure range of $\sim$8 kbar with a maximum T_{SC} of $\sim$0.7 K at $\sim$13 kbar which appears to occur within

the ferromagnetic phase and persists up to the critical pressure $P_c \simeq 16$ kbar at which T_C vanishes [4, 5]. In all of these studies, superconductivity was observed in high-purity single-crystal specimens of $CeIn_3$, $CePd_2Si_2$, and UGe_2, and it was suggested that high-purity single crystals were required to observe pressure-induced superconductivity near the critical pressure where the magnetic order vanishes. For instance, measurements were performed on single-crystal samples of UGe_2 with residual resistivities of a few tenths of a $\mu\Omega$ cm (although it was also mentioned in references [4, 5] that superconductivity had also been observed in single-crystal specimens with residual resistivities as high as 1–2 $\mu\Omega$ cm at $P \sim 13$ kbar).

In this letter, we report the results of our recent studies of polycrystalline samples of the ferromagnetic compound UGe_2 with residual resistivities as high as ~ 3 $\mu\Omega$ cm, about an order of magnitude larger than that of the purest single-crystal UGe_2 specimens previously studied. Our experiments on polycrystalline UGe_2 samples also reveal pressure-induced superconductivity and a T–P phase diagram very similar to those of the single-crystal specimens of UGe_2. These findings suggest that the pressure-induced superconductivity in UGe_2 that coexists with the ferromagnetism is relatively insensitive to the presence of impurities and defects, at least up to the levels encountered in the present experiments. These results may have important implications regarding the nature of superconductivity in UGe_2 and, in particular, raise the question of whether the superconductivity is p wave in nature. For example, in the compound Sr_2RuO_4, for which there is evidence of p-wave superconductivity [6–8], the superconducting critical temperature of ~ 1 K in the purest specimens is destroyed by impurities (presumably, Al) at the level of 1 $\mu\Omega$ cm [9] at which the electron mean free path is comparable to the superconducting coherence length. A possible scenario for UGe_2 is that the superconductivity is s wave in nature, and that it coexists with ferromagnetism in a spatially inhomogeneous way. Evidence for an inhomogeneous distribution of superconductivity and ferromagnetism has been found previously [10–12] in the ferromagnetic superconductors $ErRh_4B_4$ and $HoMo_6S_8$, in a narrow temperature range above the re-entrant superconducting transition back to the normal state at the second critical temperature $T_{SC1} < T_{SC2}$, where T_{SC1} is the superconducting critical temperature below which the sample first becomes superconducting. Our measurements also reveal a feature in the electrical resistivity at a temperature of $\sim 0.6\ T_C$ which separates a high-temperature region in the phase diagram in which $\rho(T)$ exhibits power-law behaviour ($\propto T^n$) with non-Fermi liquid-like exponents $n \simeq 1.5$ and a low-temperature region where $\rho(T)$ displays Fermi liquid (FL) behaviour ($\propto T^2$), and vanishes near P_c. We have also analysed the pressure dependence of the electrical resistivity at various pressures and have determined the pressure dependence of the exponent n of the non-Fermi liquid (NFL) power-law dependence of the resistivity, the coefficient of the FL T^2-term, and the residual resistivity ρ_0.

2. Experimental details

Polycrystalline samples of UGe_2 were synthesized by arc melting stoichiometric amounts of high-purity starting materials (U, 3N7; Ge, 8N) in an ultrahigh-purity argon atmosphere with a Zr getter. Mass losses were less than 0.2%. The samples were wrapped in Ta foil, sealed under vacuum in a quartz tube with a piece of Zr foil, and annealed at 1100 °C for one week. X-ray powder diffraction measurements revealed that the specimens crystallize in the orthorhombic $ZrGa_2$ ($Cmmm$) structure with lattice parameters close to those of reference [13] with no traces of impurities. Typical sample dimensions for the electrical resistivity measurements were $0.7 \times 0.7 \times 1.0$ mm^3. Electrical contact to the sample was made by first evaporating Au pads onto the surface and then attaching Au wires using Epo-Tech H20E silver epoxy.

Measurements of the electrical resistivity at high pressures were made with a beryllium–copper piston–cylinder clamp device up to 20 kbar using Fluorinert FC75 as a pressure-transmitting medium. The pressure was inferred inductively from the superconducting transition of a Sn or Pb manometer [14] with an estimated accuracy of ± 0.5 kbar. The electrical resistivity measurements at temperatures between 1 and 300 K were made in a ^{4}He cryostat using a Linear Research LR-201 ac resistance bridge at a frequency of 16 Hz with excitation currents of 1–10 mA. Measurements of the electrical resistivity and ac magnetic susceptibility at temperatures from 0.05 K to 2.0 K were made in an SHE ^{3}He–^{4}He dilution refrigerator with a Linear Research LR 700 low-dissipation ac resistance bridge operating at a frequency of 12 Hz and an excitation current of 50 to 500 μA. The dilution refrigerator measurements were performed by stabilizing the temperature against a germanium thermometer and averaging the sample resistance for 60 s. Magnetization measurements were made in a Quantum Design MPMS magnetometer from 1.8 K to 300 K in magnetic fields up to 5.5 T.

3. Results and discussion

Magnetization measurements on UGe_2 were made at a number of fixed temperatures and are displayed in an Arrott plot [15] (M^2 versus H/M) in figure 1 (open circles). The dashed lines are fits to the data yielding the square of the saturation magnetization M^2_{sat}. The values of M^2_{sat} versus T are also shown in figure 1 (filled circles), and a Curie temperature of $T_C = 54.5$ K is derived from the extrapolation of $M^2_{sat} \longrightarrow 0$.

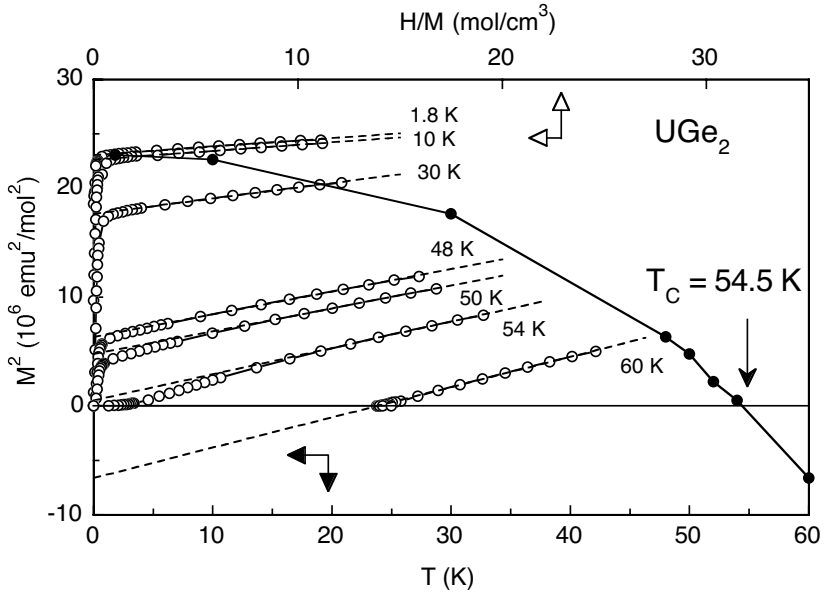

Figure 1. M^2 versus H/M (Arrott plot) for UGe_2 (open circles). The dotted lines are fits to the data yielding the square of the saturation magnetization M^2_{sat}. The filled circles show M^2_{sat} versus temperature T from which a Curie temperature of $T_C = 54.5$ K is derived.

The electrical resistivity ρ versus temperature T, at various pressures P up to 17.6 kbar, for UGe_2 is shown in figure 2. At ambient pressure, $\rho(T)$ has a weak temperature dependence above 100 K, exhibits a kink at the Curie temperature T_C of 54 K, corresponding well to the value obtained from magnetization measurements, then decreases rapidly below T_C in the

ferromagnetic state. The Curie temperature decreases monotonically with pressure as shown in inset (a) of figure 2 and the kink in ρ is no longer visible at $P = 17.6$ kbar, similar to what has been observed in previous measurements [16, 17]. For pressures between 8.8 and 14 kbar, ρ drops off rapidly at 1.0–1.2 K signalling the onset of superconductivity (SC). The superconducting transitions in four different specimens, cut from two different ingots, below 2 K at pressures of 8.8 to 12.3 kbar are shown in inset (b) of figure 2. The 90% values of the SC transitions $T_{SC}(90\%)$ occur at about 1.0 K and the 50% values $T_{SC}(50\%)$ vary non-monotonically with P from ∼0.5 K to ∼0.8 K. The apparent non-monotonic variation of $T_{SC}(50\%)$ with P probably reflects differences in T_{SC} for the four samples studied, rather than an intrinsic non-monotonic variation with P. The ac magnetic susceptibility measurements on these samples reveal a diamagnetic signal with an onset closer to $T_{SC}(50\%)$ or the temperature at which the resistivity vanishes (not shown). No superconductivity was observed above 50 mK at a pressure $P = 8.3$ kbar.

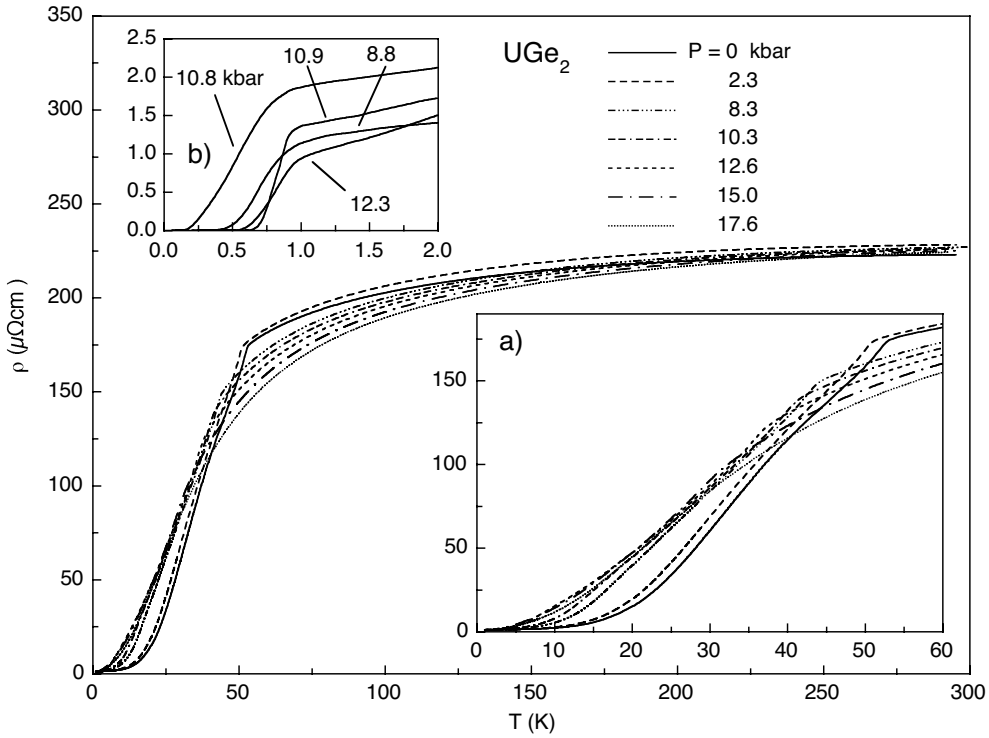

Figure 2. Electrical resistivity ρ versus temperature T for UGe_2 at various applied pressures P. Inset (a): ρ versus T below 60 K showing the decrease of the Curie temperature T_C with P. Inset (b): ρ versus T showing the superconducting transitions at various pressures between 8 and 13 kbar.

The derivative of ρ, $\mathrm{d}\rho/\mathrm{d}T$, for UGe_2 is shown in figure 3, at various pressures. We define the Curie temperature as the mid-point of the large increase in $\mathrm{d}\rho/\mathrm{d}T$ (denoted by the black arrows). Another feature is also visible in the data, defined as T_0, which corresponds to the inflection point in ρ for low pressures and a change in slope at higher pressures (results collected in table 1). Such an anomaly has also been observed in the thermal expansion coefficient [17, 18]. Neither feature is observed at 17.6 kbar, but an increase in $\mathrm{d}\rho/\mathrm{d}T$ indicating the onset of feromagnetism is observed at 15.0 kbar; therefore, we estimate the

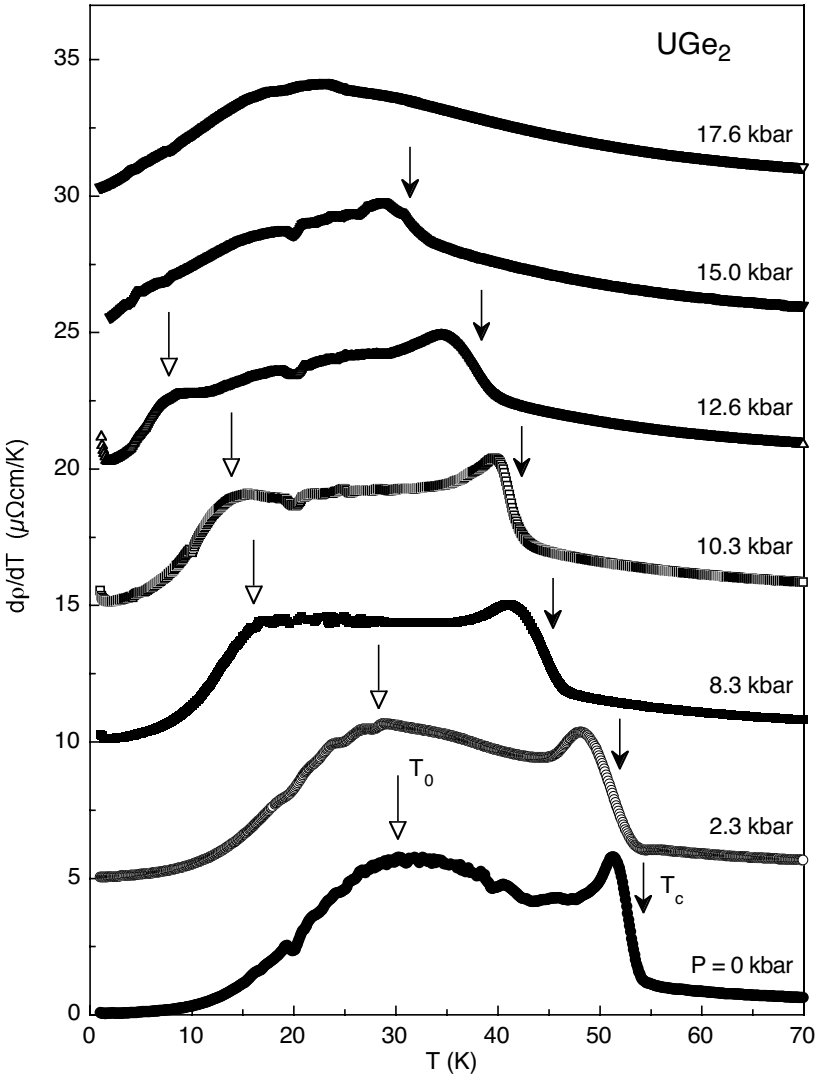

Figure 3. Derivative of the electrical resistivity $\mathrm{d}\rho/\mathrm{d}T$ versus T for UGe_2 at various applied pressures. Each curve has been shifted from the curve below it by five units for clarity. The Curie temperature T_C is defined to be the mid-point of the jump in $\mathrm{d}\rho/\mathrm{d}T$ as indicated by the black arrows. The crossover temperature T_0 is associated with the broad peak in $\mathrm{d}\rho/\mathrm{d}T$ and is indicated by the white arrows.

critical pressure P_c for the suppression of ferromagnetism to be ∼16 kbar. This value of P_c is similar to that obtained from other measurements on other polycrystalline specimens and single crystals of UGe_2 [4, 5, 16, 17].

The electrical resistivity of UGe_2 just below the Curie temperature can be described by a power law $\rho - \rho_0 = BT^n$, plotted on a log–log scale in figure 4. The lower-temperature limit of the power-law fits increases with increasing pressure and corresponds closely to the temperature T_0 of the anomaly in $\mathrm{d}\rho/\mathrm{d}T$, so it is likely that T_0 is related to a crossover boundary. The exponent n is ∼1.5–1.6 over a somewhat limited temperature range for pressures

Table 1. Physical properties of UGe_2 and fitting parameters for the electrical resistivity ρ at various applied pressures P. The Curie temperature T_C is defined as the mid-point of the jump in $d\rho/dT$. The crossover temperature T_0 is determined from the anomaly in $d\rho/dT$. The parameters B and n are extracted from the high-temperature fits of the $\rho(T)$ data to $\rho - \rho_0 = BT^n$. The parameters A and ρ_0 are derived from the low-temperature fits of the $\rho(T)$ data to $\rho = \rho_0 + AT^2$.

			High-temperature fits			Low-temperature fits		
P (kbar)	T_C (K)	T_0 (K)	B ($\mu\Omega$ cm K^{-n})	n	Fit range (K)	A ($\mu\Omega$ cm K^{-2})	ρ_0 ($\mu\Omega$ cm)	Fit range (K)
0	53	32	0.476	1.5	39–51	0.011	1.09	1.0–7.6
2.3	51	30	0.446	1.5	36–50	0.015	1.14	1.0–7.2
8.3	44	17	0.397	1.6	25–43	0.031	1.16	1.0–6.4
10.3	41	16	0.415	1.6	17–40	0.041	1.18	1.4–5.3
12.6	38	9	0.450	1.6	11–35	0.084	1.22	1.4–4.6
12.7	37	8	0.417	1.6	11–36	0.092	1.21	1.4–4.3
15.0	31	—	0.203	1.8	1–20	0.145	0.82	1.0–7.2
17.6	—	—	0.125	2.0	1–19	0.113	0.69	1.0–18.5

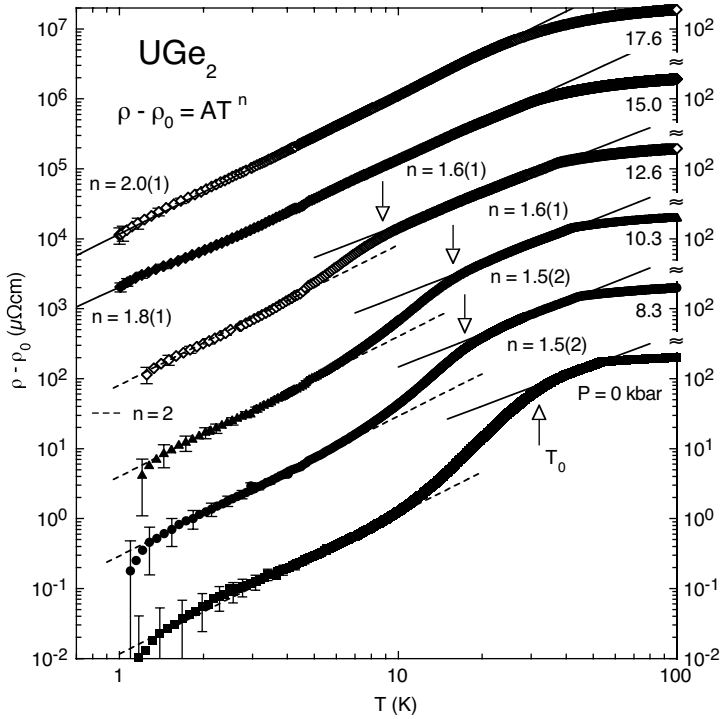

Figure 4. $\rho - \rho_0$ versus T on a log–log scale for UGe_2 at various pressures. Each curve has been shifted from the curve below it by one decade for clarity (the absolute scale is indicated on the right-hand axis). The crossover temperature T_0 was determined from the anomaly in $d\rho/dT$ (see figure 3). The solid lines are power-law fits of the $\rho(T)$ data below the Curie temperature to the expression $\rho - \rho_0 = BT^n$, where ρ_0 is an adjustable residual resistivity. The dashed lines are power-law fits of the expression above to the $\rho(T)$ data at low temperatures with an exponent $n = 2$. The values of ρ_0 were chosen to give the best fit to a T^2-power law at low temperatures. The power-law fits between T_0 and T_C were insensitive to the choice of ρ_0. The uncertainties in the last digit of the exponent n are given in parentheses.

up to 13 kbar and increases to $n \sim 1.8$ from 1 to 20 K at 15 kbar (with possible slight deviations below 3 K). The parameters of the fits to $\rho(T)$ are listed in table 1. At temperatures below 10 K within the ferromagnetic phase, the $\rho(T)$ data can be fitted by the expression $\rho(T) = \rho_0 + AT^2$ as shown in figure 5. Least-squares fits to the resistivity data of a power law $\rho - \rho_0 = BT^n$ with a fixed exponent $n = 2$ at low temperatures are shown in figure 4, indicating that the $\rho(T)$ data are consistent with a T^2-dependence within experimental error. The A-coefficient increases substantially with applied pressure as is apparent from the slope of the $\rho(T)$ curves. A plot of A versus P is shown in the inset of figure 5 which reveals that A exhibits a maximum near (but below) the critical pressure. This behaviour is consistent with previous $\rho(P, T)$ measurements on UGe_2 [4, 17]. Using the empirical relation between A and the electronic specific heat coefficient γ under pressure [19, 20], the effective mass deduced from the resistivity measurements is consistent with the enhanced γ at $P = 11$ kbar [5]. The largest value of A corresponds to an effective mass $m^* \sim 50\ m_e$ indicating that the effective mass of UGe_2 is approaching a value found in many heavy-fermion systems. The residual resistivity ρ_0 is roughly constant at 1 $\mu\Omega$ cm up to 10 kbar and then exhibits a narrow peak with a maximum value of 1.8 $\mu\Omega$ cm at 11 kbar with a width of 3 kbar near the pressure where T_{SC} is maximum as shown in the inset of figure 5 (fit results are listed in table 1).

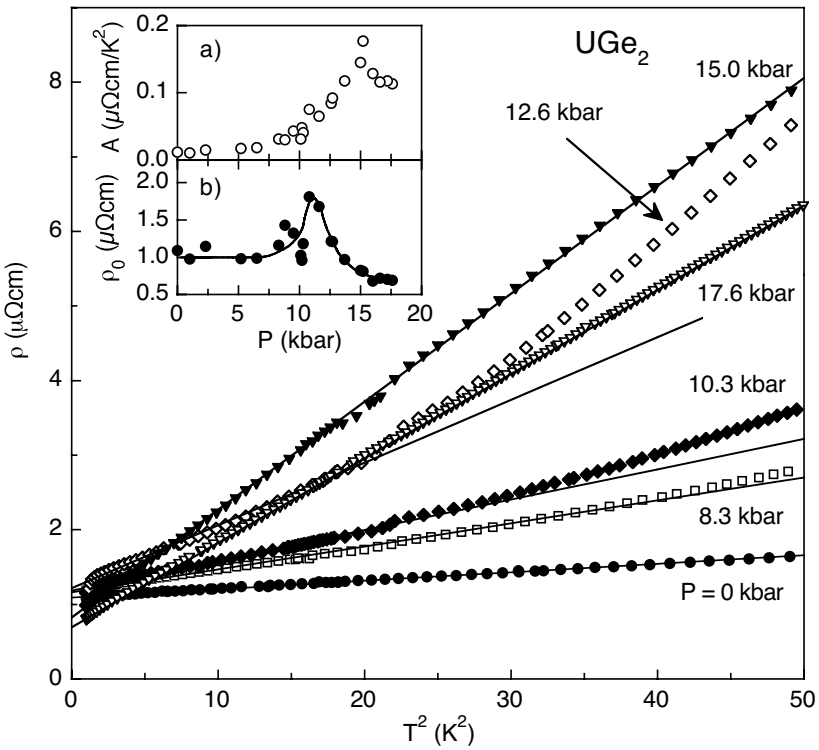

Figure 5. ρ versus T^2 for UGe_2 at various applied pressures P. The lines are fits to the data of the form $\rho = \rho_0 + AT^2$. Inset (a): coefficient of the T^2-term of $\rho(T)$, A, versus P. Inset (b): residual resistivity ρ_0 versus P.

The temperature–pressure (T–P) phase diagram for UGe_2, based on resistivity measurements under pressure, is shown in figure 6. The Curie temperature decreases monotonically with pressure P, and no resistive anomaly associated with this transition is observed above

16 kbar. The resistivity ρ follows a power-law temperature dependence with a non-Fermi liquid-like (NFL-like) exponent $n \sim 1.6$ ($n = 1.8$ at 15 kbar) for temperatures just below the Curie temperature, the range of which increases with applied pressure. Because of the NFL-like power-law behaviour of $\rho(T)$ observed in this region, we denote this region as 'NFL?' in figure 6. The temperature scale T_0 serves as a crossover boundary that separates the 'NFL?' region and a Fermi liquid region at lower temperatures where $\rho(T)$ follows a T^2-dependence, which we refer to as a ferromagnetic Fermi liquid (FMFL) state. For pressures above P_c, the system behaves as a non-magnetic Fermi liquid (NMFL). Superconductivity is observed in the pressure range 8.8 kbar $\leqslant P \leqslant$ 14 kbar with an onset temperature $T_{SC}^{onset} = 1.0$–1.2 K and $T_{SC} = 0.5$–0.8 K, as shown in the inset of figure 6. Previous studies have shown that superconductivity is suppressed to $T = 0$ K at the critical pressure and no SC was observed above P_c [4, 5].

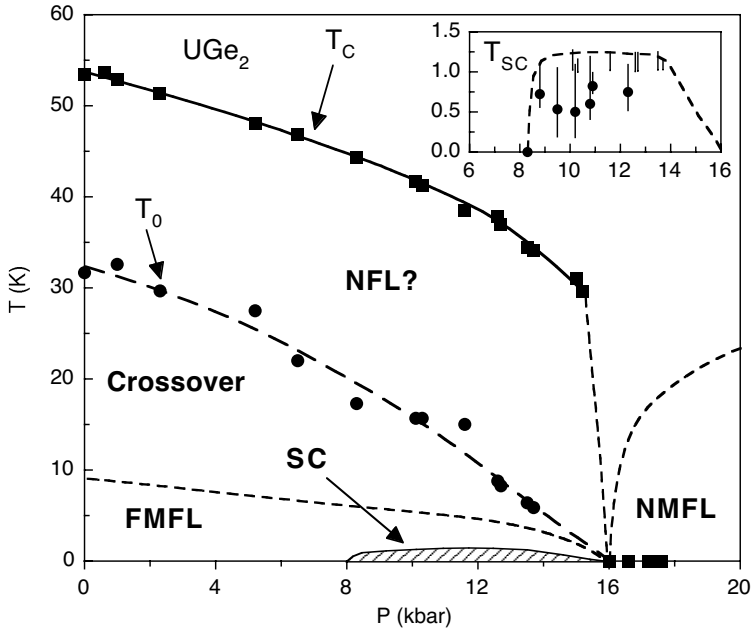

Figure 6. The temperature–pressure (T–P) phase diagram of UGe_2. 'NFL?': non-Fermi liquid; FMFL: ferromagnetic Fermi liquid; NMFL: non-magnetic Fermi liquid; SC: superconducting region. The critical pressure P_c is estimated to be ~16 kbar. The dashed lines above the FMFL and NMFL correspond to the upper range of the fits of the $\rho(T)$ data to the expression $\rho = \rho_0 + AT^2$ and are guides to the eye. Inset: expanded view of the superconducting region. The filled circles are the $T_{SC}(50\%)$ values and the upper and lower bars indicate the T_{SC}^{onset} and $T_{SC}(10\%)$ values of the superconducting critical temperature, respectively. The dashed line is a guide to the eye.

The resistivity measurements on polycrystalline samples of UGe_2 under pressure are similar to those of single-crystal specimens [4,5,17]. Our findings compare well with the results on single crystals as regards the general features of the phase diagram (monotonic decrease of T_C, crossover in behaviour at T_0, occurrence of superconductivity in a narrow pressure range) and also the magnitude of the T^2-coefficient of the resistivity, A, at low temperatures. However, there are some notable differences. The Curie temperature versus pressure curve of the polycrystalline samples exhibits an abrupt decrease near the critical pressure (figure 6), reminiscent of a first-order transition to a non-magnetic state, whereas the $T_C(P)$ curve of

single-crystal specimens is somewhat smoother [4]. However, this difference could be due to the particular method of defining the Curie temperature from the $\rho(T)$ curves. The residual resistivity ρ_0 of the polycrystalline specimens is of the order of 1–2 $\mu\Omega$ cm at ambient pressure which is nearly 5–10 times that of the purest single crystals reported in references [4, 5, 17]. A simple calculation of the mean free path l, assuming a spherical Fermi surface,

$$l = \frac{3}{e^2 N(E_F) v_F \rho_0}$$

where $N(E_F)$ (=20.33/eV cell [22]) is the density of states at the Fermi level E_F (=7.13 eV) and v_F (=1.59 $\times$ 10^8 cm s^{-1}) is the Fermi velocity yields $l \sim 150$ Å, using $\rho_0 = 1$ $\mu\Omega$ cm. A better estimate of the mean free path incorporating de Haas–van Alphen measurements [21] and band-structure calculations [22] gives $l \sim 300$ Å. At $P \simeq 12$ kbar, ρ_0 is $\sim$1.5 $\mu\Omega$ cm, implying an even shorter mean free path at pressures where superconductivity is observed. Therefore, the mean free path in these polycrystalline samples of UGe_2 is comparable to the superconducting coherence length ξ estimated to be 130–200 Å from upper-critical-field measurements [4, 5]. We also observed superconductivity with an onset of 1.2 K at $P = 10$ kbar in an unannealed polycrystalline UGe_2 sample with a residual resistivity $\rho_0 = 2.8$ $\mu\Omega$ cm (at $P = 12.6$ kbar; $\rho_0 = 3.1$ $\mu\Omega$ cm at $P = 0$ kbar) corresponding to a mean free path $l \sim 100$ Å. However, it is also possible that the observed superconductivity is filamentary and the polycrystalline samples are a collection of single-crystal grains with residual resistivities mainly due to scattering off the grain boundaries.

It appears that in most of the systems which exhibit the coexistence of ferromagnetism and superconductivity, the two phenomena form a spatially inhomogeneous mixture; in other words, they only coexist with each other on a macroscopic scale. The well known ferromagnetic superconductors $ErRh_4B_4$ and $HoMo_6S_8$ exhibit re-entrant superconductivity, i.e., the materials become superconducting below an upper critical temperature T_{SC1} and then lose their superconductivity below a lower critical temperature T_{SC2} that is below the Curie temperature T_C with the coexistence region occurring in a narrow region above T_{SC2} (for a review see references [23, 24]). Neutron scattering measurements provide evidence for the formation of an oscillatory magnetic state with a wavelength of $\lambda \sim 100$ Å [10–12] that coexists microscopically with the superconductivity. Anderson and Suhl predicted the existence of such an oscillatory magnetic state based on the exchange interaction between the localized magnetic moments associated with the f electrons and the spins of the conduction electrons [25]. Blount and Varma [26] and others [27–29] showed that such a magnetic state (in addition to other more complex FM states [29–32]) could arise as a result of the electromagnetic interaction. The regions within which the superconductivity and the oscillatory magnetic states coexist microscopically appear to coexist macroscopically with ferromagnetic regions. In these materials, the ferromagnetism involves the localized f electrons of the rare-earth constituent (Er or Ho), whereas the superconductivity is believed to be primarily associated with the d electrons of the transition metal constituent (Rh or Mo). The compound $AuIn_2$ also exhibits the simultaneous existence of ferromagnetism and superconductivity [33], but it is the nuclear moments which are ferromagnetically aligned, constituting a somewhat different situation since the coupling between the nuclear spins and the conduction electrons is extremely weak. Other FM superconductors include $ErNi_2B_2C$ [34] and $RuSr_2GdCu_2O_8$ [35,36], but the coexistence of the two phenomena in these two compounds has not yet been verified. As most of these materials contain an inhomogeneous mixture of ferromagnetism and superconductivity, it is conceivable that this is also the case for UGe_2. However, an important distinction is that UGe_2 appears to be an itinerant ferromagnet in which the same set of electrons may be responsible for both the ferromagnetism and the superconductivity.

Tateiwa *et al* measured the heat capacity under pressure in the SC state of UGe_2 and found a specific heat jump $\Delta C/\gamma T_{SC} \sim 0.2$–$0.3$, which is small compared to the BCS value of 1.43, along with a large residual electronic specific heat coefficient $\gamma_0 \sim 70$ mJ mol^{-1} K^{-2} [5]. These results could be consistent with p-wave superconductivity in which the SC order parameter vanishes at nodes on the Fermi surface, giving rise to a finite density of states in the superconducting state. On the other hand, the results also suggest the possibility that FM and SC coexist on a macroscopic scale. If one assumes that a normal (ferromagnetic) phase (with $\gamma_N = 70$ mJ mol^{-1} K^{-2}) and a superconducting phase (with $\gamma_{N'} = 30$ mJ mol^{-1} K^{-2}) contribute to the density of states, then the small fraction of the superconducting phase ($\sim$30%) is consistent with the reduced specific heat jump at T_{SC}. Indeed, estimating the jump to be $\Delta C/T_{SC} \sim 20$ mJ mol^{-1} K^{-2}, we obtain $\Delta C/(\gamma_{N'} T_{SC}) \simeq 0.67$, about half of the BCS value $\Delta C/\gamma T_{SC} = 1.43$. Neutron diffraction measurements [37] under pressure on UGe_2 reveal no change in the ordered moment below T_{SC} which indicates the coexistence of superconductivity within the FM state. These results are consistent with triplet spin pairing of superconducting electrons, an inhomogeneous mixture of ferromagnetism and superconductivity in which the magnetic moment does not change significantly at the onset of superconductivity, a sinusoidally modulated magnetic state that coexists with superconductivity, or the formation of a spontaneous vortex lattice. As described in a recent paper by Huxley *et al* [37], an estimate of the wavevector associated with the lattice parameter of the spontaneous vortex lattice can be made using the saturation magnetization at $T = 1.8$ K of $M_{sat} = 0.9\mu_B$/U atom. Assuming a lattice of closely packed vortices, this corresponds to a wavelength of about 600 Å and a wavevector of 0.01 Å^{-1}, which should be easily resolved by small-angle neutron scattering. However, the change in magnetization upon entering the superconducting state would be negligible since the penetration depth, typically of the order of 10^4 Å, is much larger than the lattice parameter of the spontaneous vortex lattice.

Recently, Blagoev *et al* [38] proposed s-wave superconductivity within a weak ferromagnet based on a theory of FM spin fluctuations with a phase diagram remarkably similar that of UGe_2 as shown in figure 6, which includes s-wave SC in a narrow region of pressure below P_c, a NFL regime just below the Curie temperature above a low-temperature FL regime, and p-wave SC above P_c. However, no superconductivity has been observed above P_c in UGe_2. Triplet (p-wave) superconductors are believed to be more sensitive to non-magnetic impurities than singlet (s-wave) superconductors. In Sr_2RuO_4, a candidate for exhibiting triplet SC [6–8, 39], superconductivity is destroyed when the impurity level rises above a value equivalent to $\rho_0 \sim 1$ $\mu\Omega$ cm [9] corresponding to an electron mean free path l of the order of (or less than) the coherence length ξ. Our results indicate that in polycrystalline specimens of UGe_2, the impurity level is such that $l \lesssim \xi$, and therefore raise the question of whether the superconductivity is p wave in nature. If one assumes the rate of depression of T_{SC} with impurity concentration (or ρ_0) at a given pressure to be similar to that of Sr_2RuO_4, $\mathrm{d}(T_{SC}/T_{SC0})/\mathrm{d}(\xi/l) = 1$ (i.e., $T_{SC}/T_{SC0} = 0$ at $\xi/l = 1$), a coherence length of 150 Å, and mean free path obtained from de Haas–van Alphen measurements $l = 300$ Å (for $\rho_0 = 1$ $\mu\Omega$ cm), a significant suppression of superconductivity is expected for samples with impurity levels of $\rho_0 = 1$ $\mu\Omega$ cm ($T_{SC}/T_{SC0} = 0.5$) and a complete suppression of superconductivity in samples with residual resistivities greater than $\rho_0 \sim 2$ $\mu\Omega$ cm. This is contrary to our results in which we observe relatively little change in the superconducting properties in samples with $\rho_0 = 1$–3 $\mu\Omega$ cm. It is possible that the estimate of the mean free path is too low and the actual mean free path is closer to $l = 1000$ Å (for $\rho_0 = 1$ $\mu\Omega$ cm). However, we would still expect a significant change in T_{SC} with the impurity levels observed in these polycrystalline specimens. On the other hand, the rate of depression of superconductivity of polycrystalline specimens of UGe_2 is not inconsistent with another possible p-wave superconductor, UPt_3, in which

superconductivity is destroyed in samples with residual resistivities of the order of $\rho_0 \sim 10$–$20\ \mu\Omega$ cm, corresponding to $\xi/l \sim 6$–7 [40]. If the rate of depression of T_{SC} of UGe_2 were comparable to that of UPt_3, $d(T_{SC}/T_{SC0})/d(\xi/l) = 0.16$ (i.e., $T_{SC}/T_{SC0} = 0$ at $\xi/l = 6$), the superconductivity in UGe_2 should be completely suppressed at impurity levels corresponding to $\rho_0 \sim 10$–$12\ \mu\Omega$ cm. To further address this issue, we are investigating the effects of Sc and Th substitutions on the observed superconductivity in UGe_2 to determine the impurity level at which the superconductivity vanishes. In addition, the relative insensitivity of the superconductivity to the scattering of electrons by defects and impurities of UGe_2 is similar to that observed in other heavy-fermion superconductors such as UBe_{13} [41,42], URu_2Si_2 [43,44], UPd_2Al_3 [45], and $CeTIn_5$ (T = Rh [46], Co [47]). For instance, $CeRhIn_5$ is an AFM pressure-induced superconductor with a $T_{SC} = 2.1$ K at 20 kbar. The residual resistivity ρ_0 of $CeRhIn_5$, which is less than 1 $\mu\Omega$ cm at ambient pressure, reaches a maximum value of $\sim$12 $\mu\Omega$ cm at the pressure at which T_{SC} is maximum [46], similar to what is observed in UGe_2.

4. Conclusions

We have measured the electrical resistivity under applied pressure of polycrystalline samples of the ferromagnetic compound UGe_2. The Curie temperature T_C decreases monotonically with applied pressure and the feature in $\rho(T)$ associated with the ferromagnetism is no longer observed above a critical pressure of $P_c \sim 16$ kbar. The resistivity exhibits a power-law temperature dependence just below T_C of the form $\rho - \rho_0 \propto T^n$ with $n \sim 1.5$–1.8 and is consistent with T^2-behaviour at lower temperatures. Superconductivity is observed within the ferromagnetic state for pressures between 8 and 14 kbar with a maximum onset temperature of 1.2 K at $\sim$13 kbar. The residual resistivity of the polycrystalline samples studied is as high as $\rho_0 \simeq 3\ \mu\Omega$ cm, indicating that the electron mean free path is smaller than or of the order of the superconducting coherence length. The relative insensitivity of the superconductivity to impurities raises the question of whether or not the superconductivity observed in the ferromagnetic phase of UGe_2 is due to triplet spin pairing.

We would like to thank J Petricka and W D Bauer for help in sample preparation. MBM would like to thank Professor H von Löhneysen and the members of the Physikalisches Institut, Universität Karlsruhe, for their hospitality during the period when part of this manuscript was prepared and the Alexander von Humbolt Foundation for a Senior Scientist Award. Useful discussions with Professors K Bedell, H von Löhneysen, and H Suhl, and Dr C Pfleiderer are gratefully acknowledged. This work was supported by the US Department of Energy under Grant No DE FG03-86ER-45230 and by the National Science Foundation under Grant No DMR00-72125.

References

[1] Mathur N D, Grosche F M, Julian S R, Walker I R, Freye D M, Haselwimmer R K W and Lonzarich G G 1998 *Nature* **394** 39

[2] Walker I R, Grosche F M, Freye D M and Lonzarich G G 1997 *Physica* C **282** 303

[3] Grosche F M, Lister S J S, Carter F V, Saxena S S, Haselwimmer R K W, Mathur N D, Julian S R and Lonzarich G G 1997 *Physica* B **239** 62

[4] Saxena S S, Agarwal P, Ahllan K, Grosche F M, Haselwimmer R K W, Steiner M J, Pugh E, Walker I R, Julian S R, Monthoux P, Lonzarich G G, Huxley A, Sheikin I, Braithwaite D and Flouquet J 2000 *Nature* **406** 587

[5] Tateiwa N, Kobayashi T C, Hanazono K, Amaya K, Haga Y, Settai R and Ōnuki Y 2001 *J. Phys.: Condens. Matter* **13** L17

[6] Ishida K, Mukuda H, Kitaoka Y, Asayama K, Mao Z Q, Mori Y and Maeno Y 1998 *Nature* **396** 658
[7] Luke G M, Fudamoto Y, Kojima K M, Larkin M I, Merrin J, Nachumi B, Uemura Y J, Maeno Y, Mao Z Q, Mori Y, Nakamura H and Sigrist M 1998 *Nature* **394** 558
[8] Ishida K, Mukuda H, Kitaoka Y, Asayama K, Mao Z Q, Mori Y and Maeno Y 2000 *Phys. Rev. Lett.* **84** 5387
[9] Mackenzie A P, Haselwimmer R K W, Tyler A W, Lonzarich G G, Mori Y, Nishizaki S and Maeno Y 1998 *Phys. Rev. Lett.* **80** 161
[10] Moncton D E, McWhan D B, Schmidt P H, Shirane G, Thomlinson W, Maple M B, MacKay H B, Woolf L D, Fisk Z and Johnston D C 1980 *Phys. Rev. Lett.* **45** 2060
[11] Sinha S K, Crabtree G W, Hinks D G and Mook H A 1982 *Phys. Rev. Lett.* **48** 950
[12] Lynn J W, Shirane G, Thomlinson W and Shelton W T R N 1981 *Phys. Rev. Lett.* **46** 368
[13] Boulet P, Daoudi A, Potel M, Noël H, Gross G M, André G and Bourée F 1997 *J. Alloys Compounds* **247** 104
[14] Smith T F, Chu C W and Maple M B 1969 *Cryogenics* **54** 53
[15] Arrott A 1957 *Phys. Rev.* **108** 1394
[16] Nishimura K, Oomi G, Yun S W and Ōnuki Y 1994 *J. Alloys Compounds* **213/214** 383
[17] Oomi G, Kagayama T and Ōnuki Y 1998 *J. Alloys Compounds* **271–273** 482
[18] Oomi G, Nishimura K, Ōnuki Y and Yun S W 1993 *Physica* B **186–188** 758
[19] Kadowaki K and Woods S B 1986 *Solid State Commun.* **58** 307
[20] Thompson J D, Fisk Z and Lonzarich G G 1989 *Physica* B **161** 317
[21] Ōnuki Y, Yun S W, Ukon I, Umehara I, Satoh K, Sakamoto I, Hunt M, Meeson P, Probst P-A and Springford M 1991 *J. Phys. Soc. Japan* **60** 2127
[22] Yamagami H and Hasegawa A 1993 *Physica* B **186–188** 182
[23] Maple M B and Fischer Ø (ed) 1982 *Superconductivity in Ternary Compounds II (Springer Topics in Current Physics vol 34)* (Berlin: Springer)
[24] Fischer Ø and Maple M B (ed) 1982 *Superconductivity in Ternary Compounds I (Springer Topics in Current Physics vol 32)* (Berlin: Springer)
[25] Anderson P W and Suhl H 1959 *Phys. Rev.* **116** 898
[26] Blount E I and Varma C M 1979 *Phys. Rev. Lett.* **42** 1079
[27] Ferrell R A, Bhattacharjee J K and Bagchi A 1979 *Phys. Rev. Lett.* **43** 154
[28] Matsumoto H, Umezawa H and Tachiki M 1979 *Solid State Commun.* **31** 157
[29] Greenside H S, Blount E I and Varma C M 1981 *Phys. Rev. Lett.* **46** 49
[30] Tachiki M, Matsumoto H and Umezawa H 1979 *Phys. Rev.* B **20** 1915
[31] Tachiki M 1981 *Physica* B **108** 801
[32] Kuper C G, Revzen M and Ron A 1980 *Phys. Rev. Lett.* **44** 1545
[33] Rehmann S, Herrmannsdörfer T and Pobell F 1997 *Phys. Rev. Lett.* **78** 1122
[34] Canfield P C, Bud'ko S and Cho B K 1996 *Physica* C **262** 249
[35] Pickett W E, Weht W and Shick A B 1999 *Phys. Rev. Lett.* **83** 3713
[36] Tallon J, Loram J W, Williams G V M and Bernhard C 2000 *Phys. Rev.* B **61** R6471
[37] Huxley A *et al* 2001 *Phys. Rev.* B **63** 144519
[38] Blagoev K B, Engelbrecht J R and Bedell K S 1999 *Phys. Rev. Lett.* **82** 133
[39] Maeno Y, Rice T M and Sigrist M 2001 *Phys. Today* **54** 42
[40] Dalichaouch Y, de Andrade M C, Gajewski D A, Chau R, Visani P and Maple M B 1995 *Phys. Rev. Lett.* **75** 3938
[41] Ott H R, Rudigier H, Fisk Z and Smith J L 1983 *Phys. Rev. Lett.* **50** 1595
[42] Maple M B, Chen J W, Lambert S E, Fisk Z, Smith J L, Ott H R, Brooks J S and Naughton M J 1985 *Phys. Rev. Lett.* **54** 477
[43] Palstra T T M, Menovsky A A, van den Berg J, Dirkmaat A J, Kes P H, Nieuwenhuys G J and Mydosh J A 1985 *Phys. Rev. Lett.* **55** 2727
[44] Maple M B, Chen J W, Dalichaouch Y, Kohara T, Rossel C, Torikachvilli M S, McElfresh M W and Thompson J D 1986 *Phys. Rev. Lett.* **56** 185
[45] Geibel C, Schank C, Thies S, Kitazawa H, Bredl C D, Böhm A, Rau M, Grauel A, Caspary R, Helfrich R, Ahlheim U, Weber G and Steglich F 1991 *Z. Phys.* B **84** 1
[46] Hegger H, Petrovic C, Moshopoulou E G, Hundley M F, Sarrao J L, Fisk Z and Thompson J D 2000 *Phys. Rev. Lett.* **84** 4986
[47] Petrovic C, Pagliuso P G, Hundley M F, Sarrao J L, Thompson J D and Fisk Z 2001 *Science* submitted